Trindane−Ruthenium Sandwich Complexes: An NMR and X-ray Crystallographic Study of $[(trindane)RuCl_2]_2$, $(trindane)RuCl_2[P(OMe)_3]$, and $[(trindane)_2Ru][BF_4]_2$

Hari K. Gupta, Philippa E. Lock, Donald W. Hughes, and Michael J. McGlinchey*

Department of Chemistry, McMaster University, Hamilton, Ontario L8S 4M1, Canada

Received December 18, 1996[⊗]

Trindane and $[(p\text{-cymene})RuCl_2]_2$ react in the melt to yield $[(trindane)RuCl_2]_2$ (**4**), the NMR spectra of which reveal the presence of $[\{(trindane)Ru\}_2(\mu\text{-}Cl)_3]Cl$ (**6**) in solution. The X-ray crystal structure of **4** reveals that two of the cyclopentene rings adopt *endo* envelope conformations, while the third five-membered ring is folded in an *exo* fashion to avoid a terminal chlorine in the other half of the dimer. Bridge cleavage with trimethyl phosphite gives $(trindane)RuCl_2[P(OMe)_3]$ (**8**), and the X-ray crystal structure shows that all three peripheral rings are folded such that the wingtip methylene groups are oriented toward the metal. Finally, treatment of **4** with excess trindane in the presence of $AgBF_4$ yields the dicationic sandwich compound $[(trindane)_2Ru]^{2+}\ 2BF_4^-$ (**3**).

Introduction

Triscyclopentenobenzene (or *trindane*, $C_{15}H_{18}$), the condensation trimer of cyclopentanone, is known to form a series of organometallic complexes, **1**, whereby the central aromatic ring is coordinated to a $Cr(CO)_3$, $Mo(CO)_3$, $Mn(CO)_3^+$, or $Fe(C_5H_5)^+$ fragment.[1] We have suggested that these compounds might serve as intermediates en route to *sumanene* ($C_{21}H_{12}$, **2**), which possesses an important structural motif present in C_{60}.[2]

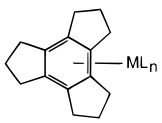

1a $ML_n = Cr(CO)_3$
1b $ML_n = Mo(CO)_3$
1c $ML_n = Mn(CO)_3^+$
1d $ML_n = Fe(C_5H_5)^+$

2

A crucial requirement of this synthesis is that the metal should activate the *exo*-benzylic hydrogens toward base-catalyzed replacement by alkyl groups, as in the steroidal example shown in Scheme 1.[3]

Since monocationic complexes, such as $[(C_6(CH_3)_6)Fe(C_5H_5)]^+$, are known to yield the corresponding $[(C_6(CH_2R)_6)Fe(C_5H_5)]^+$ systems under mild conditions,[4] we chose to attempt the preparation of the dicationic sandwich complex $[(trindane)_2Ru]^{2+}$ (**3**), in the hope that all 12 *exo*-benzylic sites could be functionalized. The most convenient route to bis(arene)ruthenium dications proceeds via the corresponding dimer $[(arene)RuCl_2]_2$; we here report the synthesis and structural characterization of $[(trindane)RuCl_2]_2$ (**4**) and its subsequent conversion to **3**.

Scheme 1. Metal-Promoted Functionalization at an *exo*-Benzylic Position

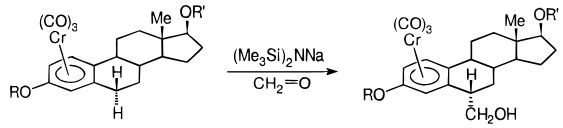

Results and Discussion

Synthetic and Spectroscopic Aspects. In continuation of our studies of organometallic derivatives of trindane,[1] we sought a route to the dicationic sandwich complex $[(trindane)_2Ru]^{2+}2BF_4^-$ (**3**). As a prelude to this goal, $[(p\text{-cymene})RuCl_2]_2$ was converted to its trisacetone derivative, which, upon treatment with trindane, yielded the mixed sandwich $[(trindane)Ru(cymene)]^{2+}2BF_4^-$ (**5**), as shown in Scheme 2. *p*-Cymene (4-isopropyltoluene) is a commonly used arene in such sandwich molecules,[5] because $[(p\text{-cymene})RuCl_2]_2$ is readily available from the redox reaction of ruthenium trichloride with dipentene, an inexpensive diene.[6]

5 was readily identified by its mass spectrum, in particular the intense peak at *m/z* 217 (the doubly-charged ion corresponding to the sandwich dication $[^{102}RuC_{25}H_{32}]^{2+}$ of mass 434). Another peak was seen at an *m/z* value of 453, which corresponds to $[(trindane)Ru(cymene)F]^+$. Moreover, the ^1H and ^{13}C NMR spectra clearly indicated the presence of the cymene ligand. Of more immediate interest were the resonances associated with the η^6-bonded trindane ligand. As seen previously in the ^1H NMR spectra of molecules

* To whom correspondence should be addressed.Phone: (905)-525-9140 ext 24504. FAX: (905)-522-2509. E-mail: mcglinc@mcmaster.ca.
⊗ Abstract published in *Advance ACS Abstracts*, September 1, 1997.

(1) Gupta, H. K.; Lock, P. E.; McGlinchey, M. J. *Organometallics* **1997**, *16*, 3628.
(2) (a) Mehta, G.; Shah, S. R.; Ravikumar, K. *J. Chem. Soc., Chem. Commun.* **1993**, 1006. (b) Sastry, G. N.; Jemmis, E. D.; Mehta, G.; Shah, S. R. *J. Chem. Soc., Perkin Trans. 2* **1993**, 1867.
(3) Jaouen, G.; Top, S.; Laconi, A.; Couturier, D.; Brocard, J. *J. Am. Chem. Soc.* **1984**, *106*, 2207.
(4) (a) Hamon, J.-R.; Saillard, J.-Y.; Le Beuze, A.; McGlinchey, M. J.; Astruc, D. *J. Am. Chem. Soc.* **1982**, *104*, 7549. (b) Valério, C.; Gloaguen, B.; Fillaut, J.-L.; Astruc, D. *Bull. Soc. Chim. Fr.* **1996**, *133*, 101.
(5) (a) Porter, L. C.; Polam, J. R. *Organometallics* **1994**, *13*, 2092. (b) Suravajjala, S.; Porter, L. C.; Polam, J. R. *Organometallics* **1994**, *13*, 37.
(6) (a) Zelonka, R. A.; Baird, M. C. *Can. J. Chem.* **1972**, *50*, 3063. (b) Bennett, M. A.; Matheson, T. W.; Robertson, G. B.; Smith, A. K.; Tucker, P. A. *Inorg. Chem.* **1980**, *19*, 1014. (c) Bennett, M. A.; Huang, T.-N.; Matheson, T. W.; Smith, A. K. *Inorg. Synth.* **1982**, *21*, 75.

S0276-7333(96)01078-3 CCC: $14.00

Scheme 2. Synthetic Routes to Trindane−Ruthenium Complexes

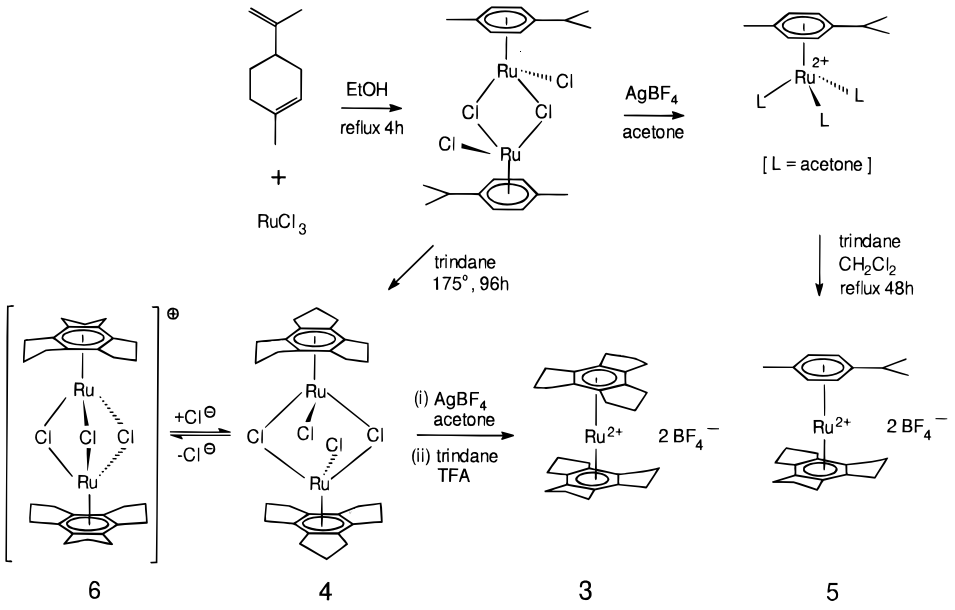

1a−**d**, complexation to a metal renders inequivalent the *exo* and *endo* faces of the $C_{15}H_{18}$ moiety and gives rise to four proton environments. The *exo* and *endo* benzylic proton absorptions are, of course, twice as intense as the central methylene (wingtip) peaks.

We have already reported the X-ray crystal structure of (trindane)$Cr(CO)_3$ (**1a**), in which all three five-membered rings adopt an envelope conformation such that the central methylene unit is folded toward the metal.[1] This molecular geometry places the *exo*-benzylic and *endo*-wingtip hydrogens in a pseudo-*trans*-diaxial relationship, and in the structurally analogous (trindane)$Mo(CO)_3$ complex, a $^3J_{H-H}$ coupling of 12.2 Hz is observed. Consequently, the *endo*-benzylic and *exo*-wingtip hydrogens occupy pseudo-equatorial sites, and, since the dihedral angle between them is approximately 90°, the $^3J_{H-H}$ value is small (~1.5 Hz).[7] The same pattern of coupling constants is observed for the trindane moiety in **5**, and so one can presume a similar *endo:endo:endo* conformation for the wingtip methylene groups, as depicted in Scheme 2.

In the absence of an appropriate commercially available cyclohexadiene precursor to trindane, it was decided to attempt an arene exchange reaction by heating [(*p*-cymene)$RuCl_2]_2$ in a large excess of molten trindane at 150 °C.[8] Gratifyingly, it is possible to obtain [(trindane)$RuCl_2]_2$ (**4**) in 85% yield. The NMR spectra and X-ray crystal structure of **4** are discussed below, but we note initially that treatment with excess trindane in the presence of $AgBF_4$ does, indeed, yield the hoped-for symmetrical sandwich dication [(trindane)$_2Ru]^{2+}2BF_4^-$ (**3**). Figure 1 shows the beautifully resolved 500 MHz ^{1}H NMR spectrum of **3**, in which coupling between all four proton environments is clearly evident. Each benzylic methylene proton appears as a doublet of doublets, while the central methylene protons (the wingtips) both exhibit the expected 18-line pattern for a doublet of triplets of triplets. The chemical shifts and coupling constants are collected in Table 1 and, again, are entirely consistent with a D_{3d} structure in which the five-membered rings adopt envelope conformations such that the wingtips are all folded inward, *i.e.*, toward the ruthenium atom.

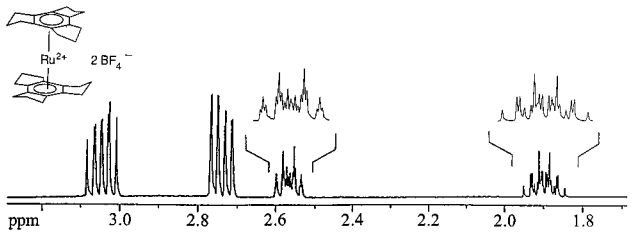

Figure 1. ^{1}H NMR spectrum of (trindane)$_2Ru^{2+}2BF_4^-$, (**3**) (500 MHz, in CD_3NO_2).

Table 1. 500 MHz ^{1}H NMR Chemical Shifts and Coupling Constants (Trindane Region) for 3−6 and 8

	δ, ppm				
^{1}H	**3**[a]	**4**[b]	**5**[a,c]	**6**[b]	**8**[b,d]
benzylic, *exo* (axial)	3.05	2.30	3.08	2.09	2.36
benzylic, *endo* (equatorial)	2.74	2.63	3.06	2.81	2.77
wingtip, *exo* (equatorial)	2.57	2.07	2.55	1.80	1.88
wingtip, *endo* (axial)	1.90	1.78	2.17	1.90	1.88
^2J(benz$_{exo}$−benz$_{endo}$)	−18.0	−15.6	*e*	−14.6	−15.3
^2J(wing$_{exo}$−wing$_{endo}$)	−13.7	−11.2	−13.7	*e*	−12.5
^3J(benz$_{exo}$−wing$_{exo}$)	8.9	7.7	7.6	*e*	8.3
^3J(benz$_{exo}$−wing$_{endo}$)	10.6	11.2	*e*	*e*	10.1
^3J(benz$_{endo}$−wing$_{exo}$)	1.5	~1	*e*	*e*	1.8
^3J(benz$_{endo}$−wing$_{endo}$)	8.8	7.9	9.4	7.5	8.6

[a] Solvent CD_3NO_2. [b] Solvent CD_2Cl_2. [c] Cymene resonances: δ 2.97 (septet, J = 6.9 Hz, 1H, Me_2CH); 1.24 (d, J = 6.9 Hz, 6H, $(CH_3)_2CH$); 2.46 (s, 3H, CH_3); 6.61 (d, J = 6.7 Hz, 2H, C*H* (aromatic)); 6.67 (d, J = 6.7 Hz, C*H* (aromatic)). [d] Methoxy resonance: δ 3.78 (d, 9H, OCH_3, $^3J(^1H-^{31}P)$ = 10 Hz). *e* Coupling constant not resolved because of overlapping multiplets.

NMR Spectra and X-ray Crystal Structures of [(Trindane)$RuCl_2]_2$ (4) and (Trindane)$RuCl_2$-[P(OMe)$_3$] (8). As discussed above, the trindane ligands in the organometallic complexes **1a**−**d**, **3**, and **5** have

(7) (a) Karplus, M. *J. Chem. Phys.* **1959**, *30*, 11. (b) Bothner-By, A. A. *Adv. Magn. Reson.* **1965**, *1*, 195. (c) Booth, H. *Prog. NMR Spectrosc.* **1969**, *5*, 149. (d) Colucci, W. J.; Jungk, S. J.; Gandour, R. D. *Magn. Reson. Chem.* **1985**, *23*, 335. (e) Breitmaier, E. *Structure Determination by NMR in Organic Chemistry*; John Wiley & Sons: Chichester, U.K., 1993; pp 42−43.

(8) It is known that complexes such as [(C_6Me_6)$RuCl_2]_2$ can be obtained by this arene exchange method: Le Bozec, H.; Touchard, D.; Dixneuf, P. H. *Adv. Organomet. Chem.* **1989**, *29*, 163.

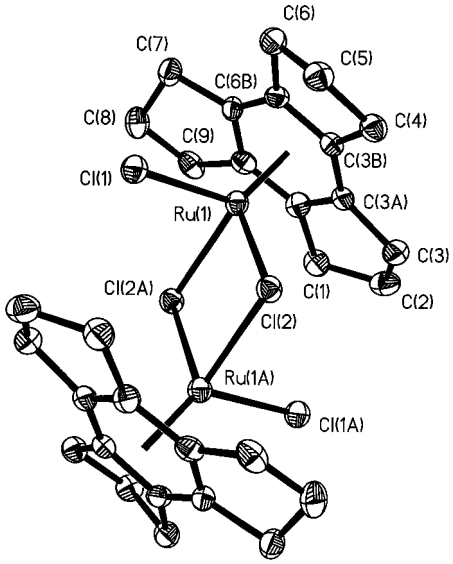

Figure 2. View of $[(C_{15}H_{18})RuCl_2]_2$ (**4**), showing the atomic numbering scheme. Thermal ellipsoids are shown at the 30% probability level and hydrogen atoms are removed for clarity. Salient bond lengths (Å) and angles (deg): Ru−(trindane centroid) 1.640, Ru(1)−Cl(1) 2.389(2), Ru(1)−Cl(2) 2.451(2), Ru(1)−Cl(2a) 2.451(2), Cl(2)−Ru(1a) 2.451(2); Cl(2)−Ru(1)−Cl(2a) 81.44(7), Ru(1)−Cl(2)−Ru(1a) 98.56(7).

been shown, either by X-ray crystallography or from their NMR data, to adopt a three-fold symmetric structure in which the five-membered ring envelopes are folded toward the metal. However, this conformation is not maintained in $[(trindane)RuCl_2]_2$ (**4**) as illustrated in the X-ray crystal structure depicted in Figure 2.

The general features of the molecule resemble those previously reported for the $[(p\text{-cymene})OsCl_2]_2$ analogue, **7**.[9] The two metals and the bridging chlorines are coplanar, with average Ru−Cl distances of 2.451 Å; the Ru···Ru distance of 3.715 Å is too long to be considered a bond. The two halves of the molecule are related by a crystallographic inversion center, and thus the two trindane ligands lie in parallel planes, and the Ru−trindane (centroid) distance is 1.640 Å. The most interesting structural feature is the intrusion of each terminal chlorine into the space occupied by the trindane *in the other half of the dimer*. This steric interaction causes one of the cyclopentene rings in each trindane ligand to fold away from the ruthenium atom, giving rise to an *endo:endo:exo* conformation for the wingtip methylene units. The space-filling representation in Figure 3 emphasizes the degree of molecular crowding in **4**.

To our surprise, the room temperature ^1H NMR spectrum of **4** in CD_2Cl_2 showed not four but eight proton environments, in the approximate ratio 4:4:2:2:2:2:1:1. Likewise, in the ^{13}C regime, the aromatic ring carbons gave rise to two resonances, while the methylene carbons exhibited a four-peak pattern. Our initial thought was that the molecule adopted C_s symmetry, as in the solid state structure. Moreover, these data suggested that one should consider the possibility of slowed arene rotation; such a phenomenon has been unequivocally demonstrated for a number of (arene)CrLL′L″ systems[10] and also in [1,4-bis(*tert*-butyl)benzene]Ru(CO)$(SiCl_3)_2$.[11]

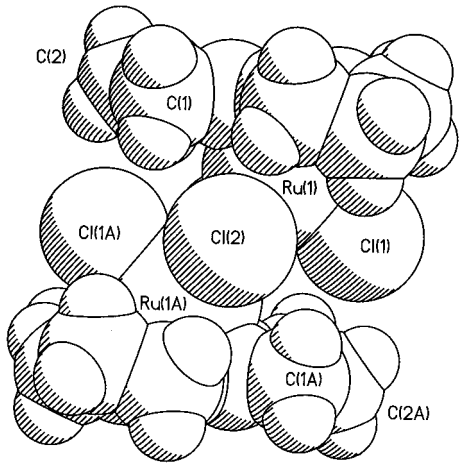

Figure 3. Crystallographic space-filling view of **4**, emphasizing the degree of crowding caused by the nonbridging chlorine atoms.

However, such a hypothesis is not valid in the case of **4**; instead, the results can be more readily explained in terms of ionization to form $[\{(trindane)Ru\}_2(\mu\text{-}Cl)_3]^+Cl^-$ (**6**). When the sample was cooled in either toluene-d_8 or CD_2Cl_2, the relative intensities of the proton resonances and of the carbon peaks gradually changed, suggesting an equilibrium between the doubly-bridged neutral molecule **4** and the triply-bridged ion **6**; the ratio of **4** to **6** is 30:70 in CD_2Cl_2 at −50 °C. Even more dramatically, use of CD_3NO_2 (which would surely favor the ionized species) resulted in almost complete conversion to only one of the isomers; at room temperature, the ratio of **4** to **6** is approximately 1:10. The $^1H-^1H$ COSY and $^1H-^{13}C$ shift-correlated spectra (Figures 4 and 5, respectively) led to the assignments collected in Table 1.

It is well established that dimeric complexes of the type $[(arene)RuCl_2]_2$ can be dechlorinated by $AgBF_4$ or HBF_4 to give the cationic species $[\{(arene)Ru\}_2(\mu\text{-}Cl)_3]^+$.[8,12] In light of the crystallographic data on **4**, one can now rationalize its facile ionization to give **6**, especially in solvents of high dielectric constant. The steric hindrance between each terminal chlorine in **4** and the trindane in the other half of the dimer is readily alleviated by loss of a chloride ion, formation of a third bridge, and adoption of a D_{3h} structure. The stability of $[\{(arene)Ru\}_2(\mu\text{-}Cl)_3]^+$ cations is evidenced not merely by X-ray crystallographic data and molecular orbital analyses[12] but also by the magnitude of the $[M - Cl]^+$ ion in the mass spectrum of **4**.

(9) Watkins, S. F.; Fronczek, F. R. *Acta Crystallogr.* **1982**, *B38*, 270.

(10) (a) McGlinchey, M. J. *Adv. Organomet. Chem.* **1992**, *34*, 285. (b) Nambu, M.; Siegel, J. S. *J. Am. Chem. Soc.* **1988**, *110*, 3675. (c) Downton, P. A.; Sayer, B. G.; McGlinchey, M. J. *Organometallics* **1992**, *11*, 3281. (d) Downton, P. A.; Mailvaganam, B.; Frampton, C. S.; Sayer, B. G.; McGlinchey, M. J. *J. Am. Chem. Soc.* **1990**, *112*, 27. (e) Kilway, K. V.; Siegel, J. S. *J. Am. Chem. Soc.* **1991**, *113*, 2332. (f) Kilway, K. V.; Siegel, J. S. *J. Am. Chem. Soc.* **1992**, *114*, 255. (g) Chudek, J. A.; Hunter, G.; MacKay, R. L.; Fäber, G.; Weissensteiner, W. *J. Organomet. Chem.* **1989**, *377*, C69. (h) Kremminger, P.; Weissensteiner, W.; Kratky, C.; Hunter, G.; MacKay, R. L. *Monatsh. Chem.* **1989**, *120*, 1175. (i) Mailvaganam, B.; Frampton, C. S.; Sayer, B. G.; Top, S.; McGlinchey, M. J. *J. Am. Chem. Soc.* **1991**, *113*, 1177. (j) Howell, J. A. S.; Beddows, C. J.; O'Leary, P. J.; Yates, P. C.; McArdle, P.; Cunningham, D.; Gottlieb, H. E. *J. Organomet. Chem.* **1997**, *527*, 21.

(11) Pomeroy, R. K.; Harrison, D. *J. Chem. Soc., Chem. Commun.* **1980**, 661.

(12) Grepioni, F.; Braga, D.; Dyson, P. J.; Johnson, B. F. G.; Sanderson, F. M.; Calhorda, M. J.; Veiros, L. F. *Organometallics* **1995**, *14*, 121.

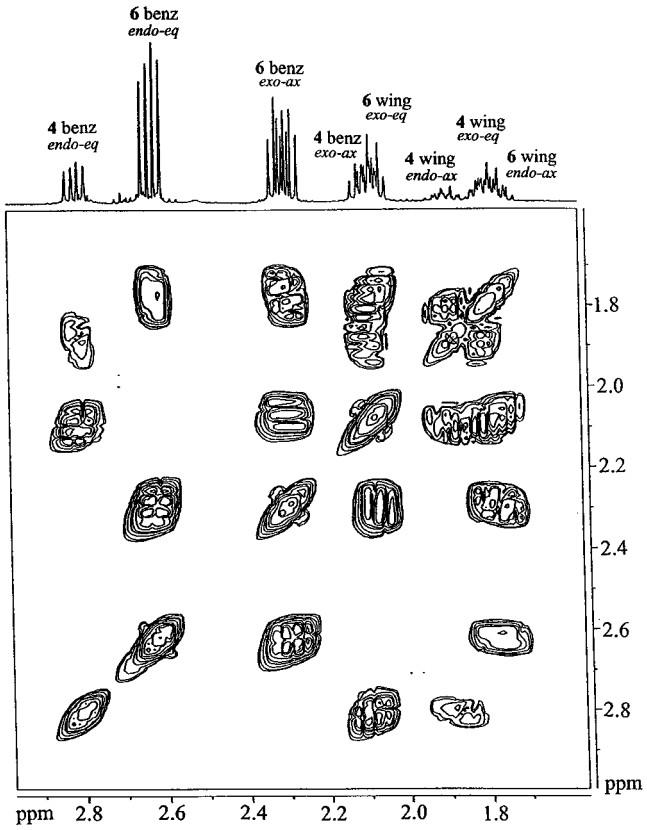

Figure 4. $^1H-^1H$ COSY spectrum of **4** and **6** (500 MHz, in CD_2Cl_2); benz = benzylic CH_2, wing = wingtip CH_2.

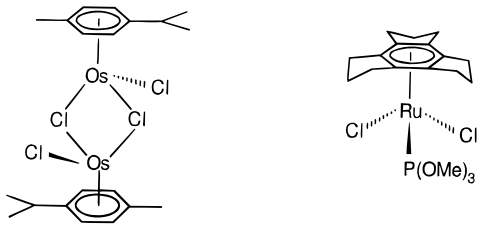

7 8

To verify that ionization of **4** is, indeed, promoted by steric hindrance from a chlorine in the other half of the dimer, **4** was treated with trimethyl phosphite with the expectation that the monomeric species (trindane)-$RuCl_2[P(OMe)_3]$ (**8**), would be formed. Figure 6 shows the X-ray crystal structure of **8**; overall, there is a close resemblance to the previously reported structures of (arene)$RuCl_2(PMePh_2)$, where the arene is benzene or cymene.[13] In particular, the $RuCl_2P$ tripod is staggered with respect to the three five-membered rings. As with the $PMePh_2$ complexes, the ruthenium−carbon distances vary such that the two lengths opposite the PR_3 ligand are significantly longer than the others (in this case, for **8**, Ru−C(3B) 2.250(4) Å and Ru−C(6A) 2.256(4) Å). It does not appear, however, that there is asymmetric bonding of the arene ligand, as none of the ring carbon atoms deviate significantly from a mean plane taken through them. For our present purposes, the most important feature is that the "normal" *endo:endo:endo* trindane conformation has been recovered. The Ru−trindane (centroid) distance is 1.719 Å (*cf.* 1.640 Å in **4**), and there appear to be no serious steric problems between the trindane wingtips and the methyls of the $P(OMe)_3$ ligand. However, the crystal packing diagram shows a weak intermolecular interaction (2.771 Å) between terminal chlorine Cl(1) and H(3a) of a neighboring trindane; the same chlorine also shows a weak interaction (2.823 Å) with H(12d), a hydrogen atom in the methoxy region of yet another molecule. The former is reminiscent of the situation in [{(toluene)-$Ru\}_2Cl_3]BF_4$.[12]

Nevertheless, the NMR spectra of **8** are not without their interesting features. The ^1H NMR spectrum of the trindane portion of **8** appears as Figure 7 and reveals that the ^{31}P nucleus clearly couples to the benzylic protons; $^4J_{P-H(exo)} = 3.8$ Hz and $^4J_{P-H(endo)} = 1.5$ Hz. Phosphorus decoupling of the ^1H spectrum yields a "conventional" trindane spectrum in which the *exo* and *endo* protons are readily assignable. The fully coupled ^{31}P spectrum is broad and featureless; presumably, it is a 490-line multiplet made up of septets of septets of decets. Selective irradiation of the *exo*-benzylic protons removes the $^4J_{P-H} = 3.8$ Hz coupling but leaves the smaller 1.5 Hz septet; the net result (Figure 8) is a slightly broadened 1:9:36:84:126:126:84:36:9:1 decet attributable to coupling to the three methyl groups.

In conclusion, **4** readily ionizes to alleviate the steric crowding caused by the proximity of a terminal chlorine in the other half of the dimer. Bridge cleavage with trimethyl phosphite gives **8**. Finally, treatment of **4** with excess trindane in the presence of $AgBF_4$ yields the dicationic sandwich compound $[(trindane)_2Ru]^{2+}$ $2BF_4^-$ (**3**) the chemistry of which will be the subject of a future report.

Experimental Section

All manipulations were carried out using standard techniques under nitrogen. Acetone was dried over molecular sieves, and all other solvents were dried and distilled by standard procedures.[14] Cyclopentanone, $AgBF_4$, and $RuCl_3 \cdot 3H_2O$ were purchased from Aldrich Chemicals Co., Inc., and used as received. Trindane was prepared as described in the literature.[15] [(*p*-Cymene)$RuCl_2]_2$ was prepared as described in the literature.[6] Mass spectra (DEI, DCI, and electrospray) were obtained on a VG analytical ZAB-SE spectrometer with an accelerating potential of 8 kV and a resolving power of 10 000. Values listed are for $^{35}Cl/^{102}Ru$ isotopomers; all peak clusters showed correct isotopic abundance patterns. NMR spectra were recorded on a Bruker DRX 500 spectrometer. ^1H and ^{13}C chemical shifts are given relative to TMS. ^1H spectral data for **3**−**6** and **8** are collected in Table 1.

Preparation of [(η^6-Trindane)Ru(η^6-cymene)][BF_4]$_2$, (5). To a solution of [(*p*-cymene)$RuCl_2]_2$ (0.200 g, 0.327 mmol) in 7 mL of dry acetone was added 0.26 g (1.33 mmol) of $AgBF_4$, and the reaction mixture was stirred for 15 min at room temperature. The reaction mixture was then transferred to a clean Schlenk flask through a cannula, one end of which was covered with filter paper, and taken to dryness under reduced pressure. Dichloromethane (10 mL) was introduced into the flask along with 0.177 g (0.89 mmol) of trindane, and the reaction mixture was refluxed for 48 h. The reaction mixture was cooled, and CH_2Cl_2 was decanted from the flask, leaving behind a light yellow viscous oil which was washed with 5 mL of CH_2Cl_2 and then with 10 mL of ether. On drying under

(13) Bennett, M. A.; Robertson, G. B.; Smith, A. K. *J. Organomet. Chem.* **1972**, *43*, C41.

(14) Perrin, D. D., Armarego, W. L. F., Perrin, D. R., Eds. *Purification of Laboratory Chemicals*, 2nd ed.; Pergamon: Oxford, 1980.

(15) (a) Mayer, R. *Chem. Ber.* **1956**, *89*, 1443. (b) Petru, F.; Galik, V. *Chem. Listy* **1957**, *51*, 2371. (c) Wallach, O. *Chem. Ber.* **1897**, *30*, 1094.

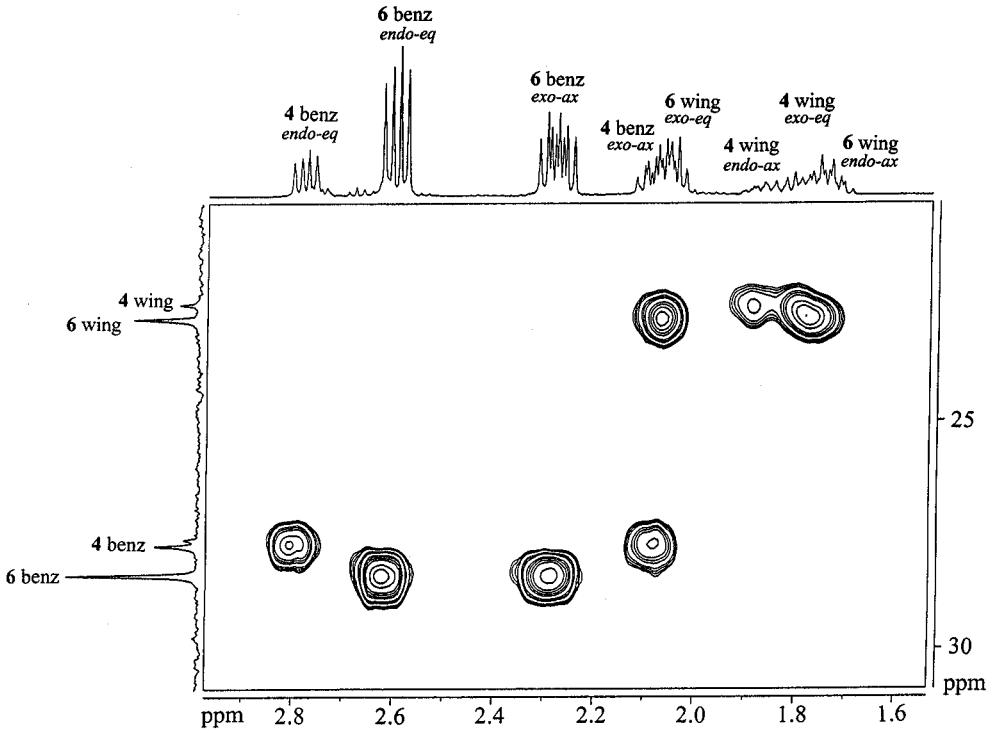

Figure 5. $^1H-^{13}C$ shift-correlated spectrum of **4** and **6** (500 MHz, 125 MHz in CD_2Cl_2); benz = benzylic CH_2, wing = wingtip CH_2.

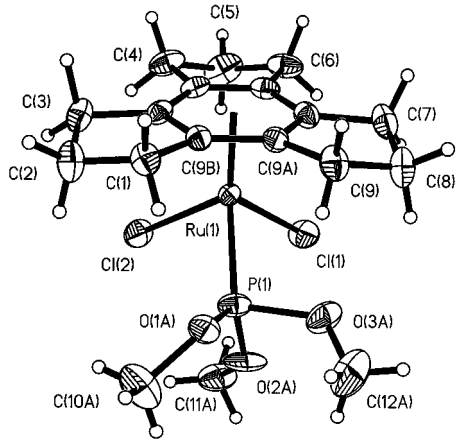

Figure 6. View of (trindane)$RuCl_2[P(OMe)_3]$ (**8**), showing the atomic numbering scheme. Thermal ellipsoids are shown at the 30% probability level, and hydrogen atoms are removed for clarity. Salient bond lengths (Å) and angles (deg): Ru−(trindane centroid) 1.719, Ru(1)−C(3A) 2.208(4), Ru(1)−C(3B) 2.250(4), Ru(1)−C(6A) 2.256(4), Ru(1)−C(6B) 2.209(4), Ru(1)−C(9A) 2.221(4), Ru(1)−C(9B) 2.220(4), Ru(1)−Cl(1) 2.402(1), Ru(1)−Cl(2) 2.415(1), Ru(1)−P(1) 2.278(1); P(1)−Ru(1)−Cl(1) 85.78(5), P(1)-Ru(1)-Cl(2) 86.93(5), Cl(1)-Ru(1)-Cl(2) 87.56(7).

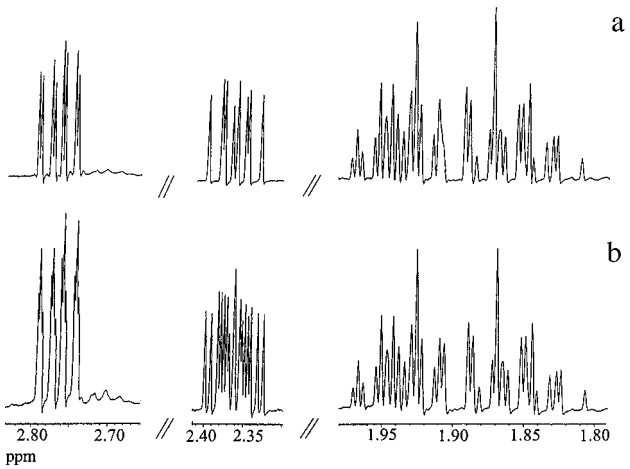

Figure 7. ^1H NMR (500 MHz, CD_2Cl_2) spectrum of the trindane region of **8**: (a) ^{31}P decoupled and (b) ^{31}P coupled.

vacuum, the oil changed to an off-white fluffy compound, **5**, (0.132 g, 0.217 mmol, 33%; mp 60 °C dec). ^{13}C NMR (125 MHz, CD_3NO_2): δ trindane, 114.8 (aromatic *C*); 30.6 (benzylic CH_2); 24.3 (wingtip CH_2); cymene: 112.2 (^{i}Pr-*C*, aromatic); 112.9 (Me-*C*, aromatic); 94.8 (*C*-H, aromatic); 92.2 (*C*-H, aromatic); 32.5 ($(Me)_2$-*C*H-); 22.9 (C-(CH_3)$_2$); 18.3 (-CH_3). Mass spectrum *m*/*z* (relative intensity): positive ion electrospray, 453 (22) [(trindane)Ru(cymene)F]$^+$, 217 (100) [$(C_{25}H_{32}Ru)$]$^{2+}$ M^{2+}. Anal. Calcd for $C_{25}H_{32}B_2F_8Ru$: C, 49.45; H, 5.31. Found: C, 49.25; H, 5.60.

Preparation of [(η^6-Trindane)$RuCl_2$]$_2$ (4) and [{(η^6-Trindane)Ru}$_2$$Cl_3$]$^+$$Cl^-$ (6). Data for **4**. A mixture of [(*p*-cymene)$RuCl_2$]$_2$ (0.205 g, 0.324 mmol) and trindane (2.0 g, 10.1 mmol) was sealed under vacuum, heated at 175 °C for 96 h, and then cooled to room temperature. To remove the large excess of unreacted trindane, the resulting red orange solid was washed with excess hexane (250 mL) and then washed with 20 mL of ether and dried *in vacuo*, to give **4** as an orange-red solid (204 mg, 0.275 mmol, 85%; mp 205 °C dec). ^{13}C NMR (125 MHz, CD_2Cl_2): δ 92.5 (*C*, aromatic); 27.8 (CH_2, (benzylic); 22.5 (CH_2, wingtip). Mass spectra *m*/*z* (relative intensity): DEI, 740 (5) [$(C_{30}H_{36}Ru_2Cl_4)$]$^+$, M^+, 705 (15) [M − Cl]$^+$, 370 (65) [(trindane)$RuCl_2$]$^+$, 298 (100) [$Ru(C_{15}H_{16})$]$^+$, 198 (75) [trindane]$^+$; DCI, 741 (5) [M + H]$^+$, 705 (55) [M − Cl]$^+$; positive ion electrospray, 705 (100) [Ru_2(trindane)$_2$$Cl]_3^+$.

Data for 6. Upon dissolution of **4** in CD_2Cl_2, there were observed two species in the ^1H and ^{13}C solution NMR spectra: these species were the neutral complex **4** and the ionized species **6**. Recording of the NMR spectra of **4** in toluene-d_8 and CD_3NO_2 supplied further evidence for the formation of the ionized species **6** in solution; in particular, from a comparison of peak intensity ratios, formation of the ionized species **6** is greatly favored in the most polar solvent, CD_3NO_2. ^{13}C NMR (125 MHz, CD_2Cl_2): δ 93.6 (*C*, aromatic); 28.4 (CH_2,

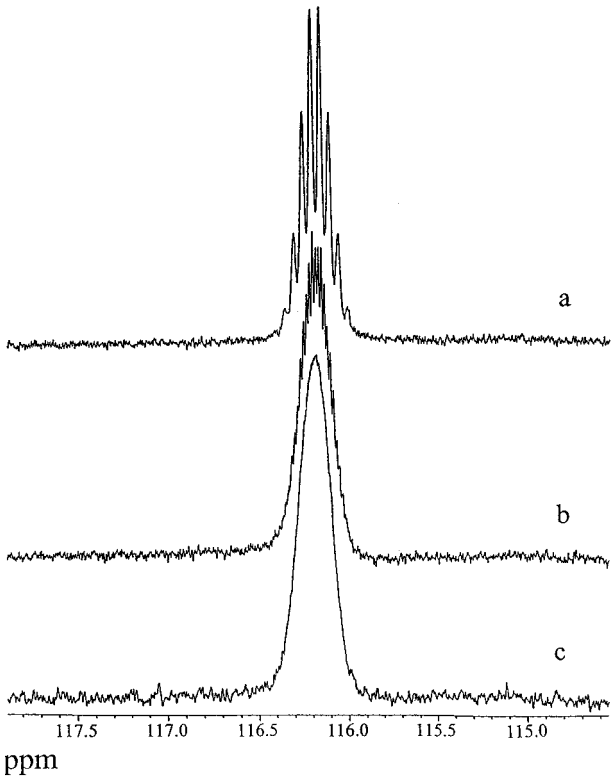

Figure 8. 202 MHz ^{31}P spectrum of **8** in CD_2Cl_2 (a) with selective decoupling of the *endo* equatorial benzylic protons and (b) the *exo* axial benzylic protons and (c) fully coupled.

benzylic); 22.8 (CH_2, wingtip). Anal. Calcd for $C_{30}H_{36}Cl_4Ru_2$: C, 48.66; H, 4.90. Found: C, 48.39; H, 5.08.

Preparation of [(η^6-trindane)$_2$Ru][BF$_4$]$_2$ (3). To 0.065 g (0.087 mmol) of [(η^6-trindane)$RuCl_2$]$_2$ in 5 mL of dry acetone was added 0.068 g (0.35 mmol) $AgBF_4$, and the reaction mixture stirred for 15 min at room temperature. The reaction mixture was then transferred to a clean Schlenk flask through a cannula, one end of which was covered with filter paper. The solution was taken to dryness under reduced pressure. Trifluoroacetic acid (3 mL) was introduced in the flask along with trindane (0.07 g, 0.36 mmol), and the reaction mixture was refluxed for 15 min and cooled to room temperature. The removal of solvent under reduced pressure gave a light yellow compound, which was washed with 10 mL of hexane and then with 10 mL of ether and then dried *in vacuo* to give **3** as a white solid (135 mg, 0.043 mmol, 49.5%; mp 210° C dec). ^{13}C NMR (125 MHz, CD_3NO_2): δ 111.9 (aromatic *C*); 29.8 (benzylic CH_2); 24.9 (wingtip CH_2). Mass spectra *m*/*z* (relative intensity): positive ion electrospray, 585 (35) [(trindane)$_2$RuBF$_4$]$^+$, 517 (10) [(trindane)$_2$RuF]$^+$, 249 (100) [(trindane)$_2$Ru]$^{2+}$. Anal. Calcd for $C_{30}H_{36}B_2F_8Ru$: C, 53.68; H, 5.41. Found: C, 53.83; H, 5.26.

Preparation of (η^6-Trindane)RuCl$_2$[P(OMe)$_3$] (8). [(Trindane)$RuCl_2$]$_2$ (74 mg, 0.1 mmol) and trimethyl phosphite (25 mg, 0.2 mmol) were taken into 10 mL of dry CH_2Cl_2, and the reaction mixture was stirred at room temperature for 3 h. The solvent was removed under reduced pressure, and the residue was washed with 3 × 5 mL of hexane and dried *in vacuo*. The red residue was recrystallized from CH_2Cl_2 to give red X-ray quality crystals of **8** (69.6 mg, 0.201 mmol, 70%; mp 165 °C). ^{13}C NMR (125 MHz, CD_2Cl_2): δ 102.9 (d, $^3J(^{13}C-^{31}P) = 4.1$ Hz, aromatic *C*); 28.6 (benzylic CH_2); 22.6 (wingtip CH_2); 54.8 (d, $^2J(^{13}C-^{31}P) = 7.9$ Hz, O-CH_3). Mass spectra *m*/*z* (relative intensity): DEI, 494 (10) [(trindane)$RuCl_2P(OMe)_3$]$^+$, 370 (10) [M − P(OMe)$_3$]$^+$, 298 (10) [Ru($C_{15}H_{16}$)]$^+$, 198 (15) [trindane]$^+$; high-resolution DEI, calculated mass for $^{12}C_{18}{}^1H_{27}{}^{16}O_3{}^{31}P{}^{35}Cl_2{}^{102}Ru$, [M]$^+$, 494.0118 amu, observed mass 494.0142 amu. Anal. Calcd for $C_{18}H_{27}O_3PCl_2Ru$: C, 43.73; H, 5.50. Found: C, 44.00; H, 5.60.

X-ray Crystallographic Analysis. X-ray intensity data for **4** were collected at 157 K with the use of graphite-monochromated Ag Kα ($\lambda = 0.560\,86$ Å) radiation on a Siemens P3 diffractometer. Data were corrected for Lorentz and polarization factors. Crystal stability was monitored by measuring three standard reflections every 97 measurements. An empirical absorption correction was based on 396 data (transmission factors 1.000 (maximum) and 0.300 (minimum)).

X-ray intensity data for **8** were collected at 300 K with the use of graphite-monochromated Mo Kα ($\lambda = 0.710\,73$ Å) radiation on a Siemens P4 diffractometer, equipped with a Siemens Smart 1K charge coupled device (CCD) area detector (using the program SMART[16]) and a rotating anode. The crystal-to-detector distance was 3.991 cm, and the data collection was carried out in 512 × 512 pixel mode, with 2 × 2 pixel binning. One hemisphere of data was collected, to better than 0.8 Å resolution. Upon completion of the data collection, the first 50 frames were recollected in order to improve the decay corrections analysis (if required). Also, redundant reflections were monitored as a function of time to check for decay. Data were processed with the use of the program SAINT,[17] which applied Lorentz and polarization corrections to three-dimensionally integrated diffraction spots. The program SADABS[18] was used to merge scans to apply decay corrections, if any, and to apply an empirical absorption correction based on redundant measurements.

Calculations were performed with the use of the SHELXTL PC[19] program library. Crystal data, data collection and reduction, and structure details for $C_{30}H_{36}Cl_4Ru_2$ (**4**) and $C_{18}H_{27}O_3Cl_2Ru$ (**8**) are listed in Table 2. Salient bond lengths and bond angles for **4** and **8** are listed in Figures 2 and 6, respectively.

X-ray Analysis for C$_{30}$H$_{36}$Cl$_4$Ru$_2$ (4). Crystals of **4** were grown from a solution of CH_2Cl_2/hexane by slow evaporation of solvent. A red crystal measuring approximately 0.43 mm × 0.24 mm × 0.08 mm was mounted on a glass fiber attached to a brass pin and aligned on the diffractometer. Unit cell parameters were determined by a least-squares fit of the angular settings of 25 reflections with $15.26° \le 2\theta \le 44.23°$. The structure was successfully solved in $P2_1/n$ (No. 14), with $a = 9.412(2)$ Å, $b = 14.991(3)$ Å, $c = 10.367(2)$ Å, $\beta = 112.41(3)°$, $V = 1352.3(5)$ Å^3, and $Z = 2$. The positions of the non-hydrogen atoms were determined by direct methods and refined anisotropically with the use of full-matrix least-squares methods. All H atoms were included with the use of a riding model; isotropic thermal parameters were set at 50% greater than those for the C atoms to which they were attached. The refinement on 1765 unique reflections (R(int) = 3.91%) from 3.94 to 40.00 in 2θ converged to $R = 7.45\%$, $R_w = 13.27\%$, and GOF = 0.904 for 163 parameters.

X-ray Analysis for C$_{18}$H$_{27}$O$_3$Cl$_2$PRu (8). Crystals of **8** were grown from a solution of CH_2Cl_2 by slow evaporation of solvent. A red crystal measuring approximately 0.20 mm × 0.12 mm × 0.04 mm was mounted on a glass pin and aligned on the diffractometer. Initial unit cell parameters were determined by a least-squares fit of the angular settings of 112 strong reflections collected by a 4.5° scan in 15 frames over three different parts of reciprocal space. After data collection, the unit cell was re-indexed on 8000 reflections. The structure was successfully solved in $P2_1/c$ (No. 14) with $a = 9.141(2)$ Å, $b = 14.931(1)$ Å, $c = 14.996(3)$ Å, $\beta = 94.58(1)°$, $V = 2040.0(6)$ Å^3, and $Z = 4$. The positions of the non-hydrogen atoms were determined by direct methods and refined aniso-

(16) SMART, version 4.05, 1996; Siemens Energy and Automotive Analytical Instrumentation, Madison, WI, 53719.
(17) SAINT, version 4.05, 1996; Siemens Energy and Automotive Analytical Instrumentation, Madison, WI, 53719.
(18) Sheldrick, G. M. SADABS (Siemens Area Detector Absorption Corrections), 1996.
(19) Sheldrick, G. M. SHELXTL, Release 5.03, 1994; Siemens Crystallographic Research Systems, Madison, WI, 53719.

Table 2. Crystal Data and Structure Refinement for 4 and 8

	4	**8**
	Crystal Data	
empirical formula	$C_{30}H_{36}Cl_4Ru_2$	$C_{18}H_{27}Cl_2O_3PRu$
fw	740.53	494.34
color, habit	red, plate	red, plate
temp, K	157(2)	300(2)
wavelength, Å	0.560 86	0.710 73
cryst syst	monoclinic	monoclinic
space group	$P2_1/n$	$P2_1/c$
a, Å	9.412(2)	9.141(2)
b, Å	14.991(3)	14.931(1)
c, Å	10.367(2)	14.996(3)
β, deg	112.41(3)	94.58(1)
volume, Å^3	1352.3(5)	2040.0(6)
Z	2	4
density (calcd), Mg/m^3	1.819	1.610
abs coeff, mm^{-1}	0.806	1.123
F(000)	744	1008
cryst size, mm	0.43 × 0.24 × 0.08	0.20 × 0.12 × 0.04
	Data Collection	
θ range for data collection, deg	1.97−20.00	1.93−30.47
limiting indices	$-12 < h < 11$, $-8 < k < 20$, $-2 < l < 14$	$-9 < h < 13$, $-21 < k < 21$, $-21 < l < 21$
no. of reflns collected	2144	21311
no. of independent reflns	1766 [R(int) = 0.0391]	5240 [R(int) = 0.0790]
	Solution and Refinement	
refinement method	full-matrix least-squares on F^2	full-matrix least-squares on F^2
data/restraints/parameters	1765/0/163	5240/0/236
goodness-of-fit on F^2	0.904	1.049
final R indices [$I > 2\sigma(I)$]	$R_1 = 0.0536$, w$R_2 = 0.1252$	$R_1 = 0.0499$, w$R_2 = 0.0869$
R indices (all data used)	$R_1 = 0.0745$, w$R_2 = 0.1327$	$R_1 = 0.0962$, w$R_2 = 0.1047$
largest diff peak and hole, e Å^{-3}	1.140 and −0.376	0.455 and −0.752

tropically with the use of full-matrix least-squares methods. All H atoms were included with the use of a riding model; isotropic thermal parameters for trindane H atoms and methyl H atoms were set respectively at 20% and 50% greater than those for the C atoms to which they were attached. The refinement on 5240 unique reflections (R(int) = 7.90%) from 3.86 to 60.94 in 2θ converged to $R = 9.62\%$, $R_w = 10.47\%$, and GOF = 1.049 for 236 parameters.

Acknowledgment. Financial support from the Natural Sciences and Engineering Research Council of Canada, and also from the donors of the Petroleum Research Fund, administered by the American Chemical Society, is gratefully acknowledged. P.E.L. thanks the Province of Ontario for a graduate scholarship. Mass spectra were obtained courtesy of Dr. Richard Smith of the McMaster Regional Centre for Mass Spectrometry. We also thank one of the reviewers for particularly insightful comments.

Supporting Information Available: Tables of atomic parameters including fractional atomic coordinates and equivalent isotropic displacement parameters, bond distances and angles, anisotropic and isotropic displacement parameters, and cell and packing diagrams for the crystal structures **4** and **8** (20 pages). Ordering information is given on any current masthead page.

OM961078K